Lung-specific loss of the laminin α3 subunit confers resistance to mechanical injury

Daniela Urich[1], Jessica L. Eisenberg[2], Kevin J. Hamill[2], Desire Takawira[2], Sergio E. Chiarella[1], Saul Soberanes[1], Angel Gonzalez[1], Frank Koentgen[3], Tomas Manghi[1], Susan B. Hopkinson[2], Alexander V. Misharin[1], Harris Perlman[1], Gokhan M. Mutlu[2], G. R. Scott Budinger[1,2,*,‡] and Jonathan C. R. Jones[1,2,*]

[1]Department of Medicine, Northwestern University Feinberg School of Medicine, Chicago, IL 60611, USA
[2]Department of Cell and Molecular Biology, Northwestern University Feinberg School of Medicine, Chicago, IL 60611, USA
[3]Ozgene Pty. Ltd, Bentley 6102, Western Australia, Australia

*These authors contributed equally to this work
‡Author for correspondence (s-buding@northwestern.edu)

Accepted 6 May 2011
Journal of Cell Science 124, 2927–2937

doi: 10.1242/jcs.080911

Summary

Laminins are heterotrimeric glycoproteins of the extracellular matrix that are secreted by epithelial cells and which are crucial for the normal structure and function of the basement membrane. We have generated a mouse harboring a conditional knockout of α3 laminin (*Lama3*$^{fl/fl}$), one of the main laminin subunits in the lung basement membrane. At 60 days after intratracheal treatment of adult *Lama3*$^{fl/fl}$ mice with an adenovirus encoding Cre recombinase (Ad-Cre), the protein abundance of α3 laminin in whole lung homogenates was more than 50% lower than that in control-treated mice, suggesting a relatively long half-life for the protein in the lung. Upon exposure to an injurious ventilation strategy (tidal volume of 35 ml per kg of body weight for 2 hours), the mice with a knockdown of the α3 laminin subunit had less severe injury, as shown by lung mechanics, histology, alveolar capillary permeability and survival when compared with Ad-Null-treated mice. Knockdown of the α3 laminin subunit resulted in evidence of lung inflammation. However, this did not account for their resistance to mechanical ventilation. Rather, the loss of α3 laminin was associated with a significant increase in the collagen content of the lungs. We conclude that the loss of α3 laminin in the alveolar epithelium results in an increase in lung collagen, which confers resistance to mechanical injury.

Key words: Laminin, Extracellular matrix, Lung, Basement membrane

Introduction

The alveolar compartment of the lung contains a unique basement membrane, which is shared by alveolar epithelial and endothelial cells. This basement membrane allows efficient transfer of oxygen and carbon dioxide between the airspaces and vasculature, and contributes to the viscoelastic properties of the lung parenchyma that are crucial for normal lung physiology (Weibel, 1963). All basement membranes comprise a complex of extracellular matrix proteins, including collagen, nidogen, heparin-sulfated proteoglycans and laminins (Martin and Timpl, 1987). Of these, laminins exhibit tissue specificity (Miner, 2008; Pierce et al., 1998; Schuger et al., 1990; Willem et al., 2002). Each laminin is a heterotrimer, composed of an α-, β- and γ-subunit. Five alpha, three beta and three gamma chains have been identified from which more than 16 combinations might exist in vivo (Miner, 2008). With regard to the lung, alveolar epithelial cells deposit a number of distinct laminin heterotrimers into their basement membrane, with some of these playing important roles in lung development (Martin and Timpl, 1987; Pierce et al., 1998). Specifically, using inhibitory or knockout strategies, investigators have shown that laminin 111 and the α5 laminin subunit are required for normal lung development (Nguyen et al., 2005; Schuger et al., 1990; Willem et al., 2002). Conversely, the α3 laminin subunit does not appear to be required for lung development because neonatal mice globally lacking α3 laminin (*Lama3*$^{-/-}$) have no obvious lung phenotype (Ryan et al., 1999). This finding is somewhat surprising because α3 laminin is the main component of the alveolar basement membrane in the adult lung (Miner, 2008; Pierce et al., 1998). However, because these mice die from a blistering skin disease very shortly after birth, the function or α3 laminin in the adult lung is not known (Ryan et al., 1999).

Unlike the basement membrane in many other organs, the alveolar basement membrane is exposed to cyclic mechanical stretch as a consequence of normal breathing. When alveolar ventilation increases, such as during exercise or stress, the degree of deformation of the basement membrane becomes larger, such that at total lung capacity the basement membrane surface area is enlarged by ~40% (Tschumperlin and Margulies, 1999). Stretch of the alveolar basement membrane can exceed this level in patients with respiratory failure who are subjected to positive pressure mechanical ventilation (Vlahakis and Hubmayr, 2005). In cultured primary rat alveolar epithelial cells, we have reported that the interaction between α3-subunit-containing laminins and the cell surface receptor dystroglycan induces signaling that might protect cells from the harmful effects of mechanical stimulation (Budinger et al., 2008). Thus, we hypothesized that in mice the loss of α3 laminin might not only alter the viscoelastic

properties of the lung but also disrupt signaling pathways activated by ventilation. To test this hypothesis, we generated a mouse with a conditional knockout of α3 laminin in the lung epithelium and subjected it to positive pressure ventilation.

Results

Generation of *Lama3* floxed mice

We generated a vector targeting exon 42 of the *Lama3* mouse gene (the murine equivalent of exon 41 of the human *LAMA3* gene) by positioning *loxP* sequences 3 kb upstream and 4 kb downstream of exon 42 (Fig. 1A). Deletion of this exon will result in loss of the two main splice isoforms encoded by the *Lama3* gene (the α3a and α3b laminin subunits) (Ryan et al., 1999). This vector was introduced into embryonic stem cells (ESCs) through electroporation, and the cells were selected and screened for homologous recombination by southern blotting. These cells were injected into blastocysts, which were then implanted into mice. The chimeric offspring were mated to C57BL/6 mice and ESC-derived progeny were sequentially bred to produce mice homozygous for the floxed α3 laminin subunit allele. To avoid the possibility that the Neo cassette, which contains strong regulatory regions, might influence expression of the targeted gene or it neighbors, we removed it by mating the homozygous floxed mice to *Flpe* mice. Mice bearing a homozygous floxed α3 laminin subunit allele in the absence of the Neo cassette were further bred to remove the *Flpe* transgene. DNA isolated from the tails of five littermates resulting from crossing animals exhibiting germline transmission of the floxed allele was digested with *Eco*RV, electrophoresed, transferred onto a nitrocellulose membrane and hybridized with a probe containing sequences 39 to the *loxP* sites (Fig. 1B). The expected size for the wild-type (wt) fragment is 26 kb and for the flox fragment is 9.8 kb. Genomic DNA was isolated from the lungs of wild-type mice infected with null virus, and *Lama3*$^{fl/fl}$ mice infected with null virus or Cre-encoding virus. PCR primers were designed to amplify within intron 40 through intron 42, a region flanking the engineered *loxP* sites. We amplified the expected 950-bp product from the wild-type lung genomic DNA and an 1100-bp product from the lung genomic DNA from *Lama3*$^{fl/fl}$ mice treated with control virus, indicating the insertion of the *loxP* sites. Using the same primers, we amplified an additional 500-bp product from lung genomic DNA from the *Lama3*$^{fl/fl}$ mice treated with Cre virus, indicating excision of the targeted sequence (Fig. 1C). To ensure that the knockdown did not result in the production of an N-terminal fragment, we designed primer sequences to amplify short regions specifically within the *Lama3a* and *Lama3b* regions and within a region common to both, downstream of the deleted exon (supplementary material Fig. S1). In RNA obtained from alveolar type II cells isolated from mice treated with Ad-Null or Ad-Cre 60 days earlier, all three products were significantly reduced confirming a knockdown of *Lama3a* and *Lama3b* and suggesting that no N-terminal laminin fragment is produced (Fig. 1D).

Lung-specific knockdown of α3 laminin

Lama3$^{fl/fl}$ mice were treated with Ad-Cre or Ad-Null and 30 days, 60 days or 6 months later the lungs were harvested, homogenized and the abundance of the α3 laminin subunit was detected by immunoblotting. Using β-galactosidase Cre reporter mice, we have previously shown that this dose of adenovirus results in widespread recombination in the airways and alveolar space of the lung (Budinger et al., 2010; Weinberg et al., 2010). Minimal

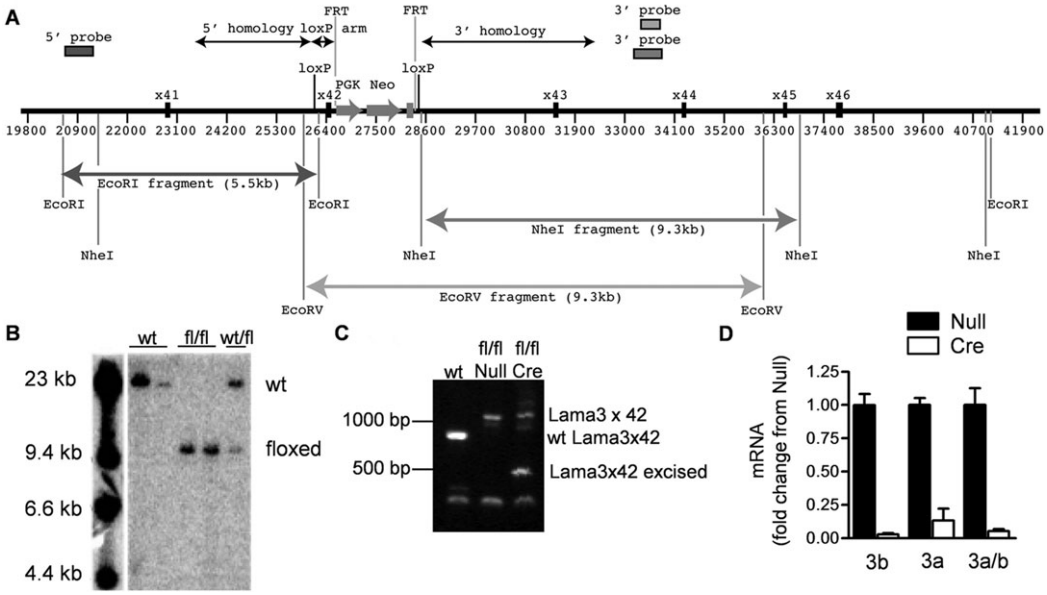

Fig. 1. Generation of the *Lama3*$^{fl/fl}$ mouse. (**A**) Diagram of part of the vector that targets exon 42 of the *Lama3* mouse gene. (**B**) DNA isolated from tails of five littermates resulting from crossing animals exhibiting germline transmission of the floxed allele was digested with *Eco*RV, electrophoresed, transferred onto a nitrocellulose membrane and hybridized with a probe containing sequences 3′ to the *loxP* sites. The expected size for the wild-type (wt) fragment is 26 kb and for the flox fragment is 9.8 kb. (**C**) Genomic DNA was isolated from the lungs of null virus-infected wild-type mice (wt), null-virus-infected *Lama3*$^{fl/fl}$ mice (fl/fl Null) and Cre virus infected *Lama3*$^{fl/fl}$ mice (fl/fl Cre) and subjected to PCR using primers flanking the engineered region. (**D**) *Lama3*$^{fl/fl}$ mice were treated intratracheally with a null adenovirus (Null) or an adenovirus encoding Cre recombinase (Cre) and 60 days later alveolar type II cells were isolated from the mice from which RNA was isolated for measurement (qRT-PCR) of short regions of the *Lama3* gene specific to *Lama3a* (3a) or *Lama3b* (3b) transcripts or those common to *Lama3a* and *Lama3b* (3a/b) (also see supplementary material Fig. S1).

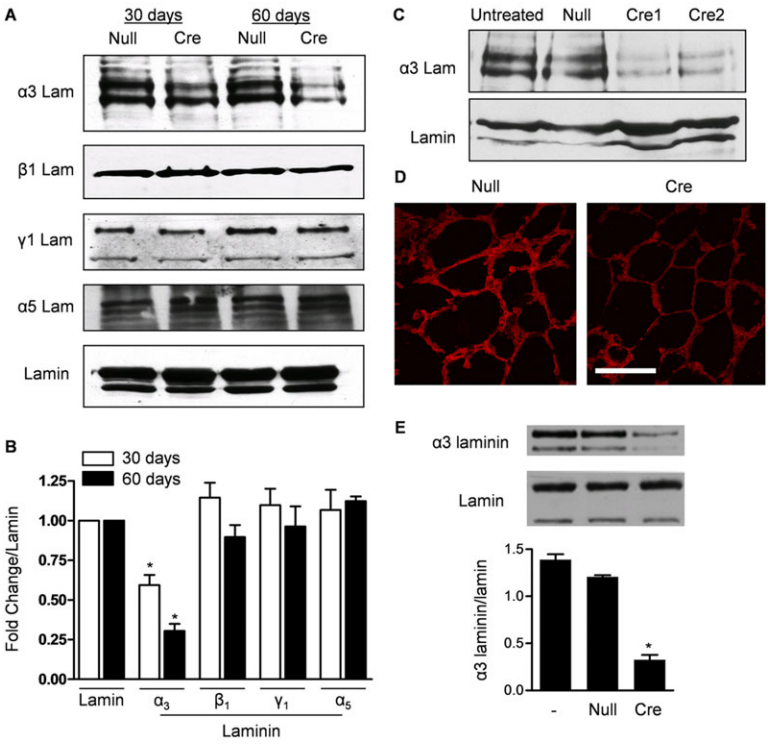

Fig. 2. The half-life of the α3 laminin subunit in the adult lung is between 30 and 60 days. (**A**) *Lama3*$^{fl/fl}$ mice were treated with a null adenovirus (Null) or an adenovirus encoding Cre recombinase (Cre), and whole lung homogenates were obtained after the indicated number of days. Extracts of the lungs from four mice treated with null virus and four mice treated with the Cre-encoding virus were analyzed by immunoblotting using antibodies against the α3, β1, γ1 and α5 laminin subunits. Lamin immunoreactivity was used as a loading control. A representative blot of the extracts is shown. (**B**) Blots were scanned for densitometry and laminin subunit levels were quantified relative to the lamin loading control. (**C**) Lung homogenates from untreated mice and mice treated 6 months earlier with Ad-Null or Ad-Cre were immunoblotted using an antibody against α3 laminin. (**D**) Frozen sections of the lungs of mice 60 days after treatment with either Ad-Null or Ad-Cre were prepared for immunofluorescence using an antiserum against mouse α3 laminin. Scale bar: 50 μm. (**E**) Alveolar type II cells were isolated from untreated mice and mice treated 60 days earlier with Ad-Null or Ad-Cre. The cells from three animals were pooled, lysed and immunoblotted using antibodies against α3 laminin and lamin (loading control) (two replicates). *P<0.05 for comparison between Null and Cre.

knockdown of α3 laminin protein was observed 30 days after the administration of adenoviral Cre recombinase (Fig. 2A,B). At 60 days after the administration of Ad-Cre, an ~60% knockdown of the α3 laminin subunit was observed in mouse lung homogenates (Fig. 2A,B). This knockdown persisted in mice maintained for 6 months after infection with adenoviral Cre (Fig. 2C). Furthermore, there was a substantial reduction in staining of sections of the lungs of the Cre-virus-treated animals compared with that observed in the control (Fig. 2D). These results suggest that the normal half-life of the α3 laminin subunit in the adult murine lung is between 30 and 60 days. To determine whether the loss of α3 laminin was associated with compensatory changes in other laminin subunits, we immunoblotted the lung homogenates using antibodies against the α5, β1 and γ1 laminin subunits (Fig. 2A). There was no obvious change in expression of these proteins. To determine whether infection of the animals with adenoviral Cre resulted in a knockdown of α3 laminin in the alveolar epithelium, we isolated alveolar type II cells from mice infected 60 days earlier with Ad-Cre or Ad-Null and measured the levels of α3 laminin in lysates of the freshly isolated cells by immunoblotting. Alveolar type II cells derived from mice infected with Ad-Cre had substantially lower levels of α3 laminin compared with cells isolated from Ad-Null infected mice (Fig. 2E).

Knockdown of the α3 laminin subunit in the adult lung is not associated with changes in gas exchange and results in minimal changes in lung mechanics

We performed arterial blood gas analysis of sedated control mice and those with knockdown of the α3 laminin subunit. No significant difference was observed in the arterial pH, or the arterial concentrations of oxygen and carbon dioxide between two groups (Table 1). We also compared baseline lung

Table 1. Baseline gas exchange and lung mechanics in control and α3-laminin-knockdown mice

Measure	Null	Cre	*P*-value
Arterial pH	7.31±0.1	7.34±0.05	0.60
Arterial PCO_2 (torr)	52±7.0	58±14	0.43
Arterial PO_2 (torr)	88.8±23.6	78.7±9.6	0.97
Quasi-static compliance (Cst) (ml/cm H_2O)	0.095±0.011	0.089±0.009	0.15
Newtonian resistance (Rn) (cm H_2O•second/ml)	0.826±016	0.397±0.214	<0.001
Resistance (R) (cm H_2O• second/ml)	0.820±0.174	0.781±0.146	0.59
Elastance (E) (cm H_2O/ml)	27.6±5.0	27.2±2.3	0.37
Inertance (I) (cm H_2O•second^2/ml)	– 0.0006±0.0003	– 0.0007±0.0004	0.86
Tissue damping (G) (cm H_2O/ml)	5.90±1.07	5.96±0.680	0.86
Tissue elastance (H) (cm H_2O/ml)	30.0±5.87	27.1±2.80	0.12
Hysteresivity (η)	0.20±0.02	0.22±0.02	0.008
Area of the PV loop (cm H_2O•ml)	4.67±2.3	5.42±3.7	0.56

Lama3$^{fl/fl}$ mice were treated with a null adenovirus (Null) or an adenovirus encoding Cre recombinase (Cre) and 60 days later arterial blood gases (arterial pH, PCO_2 and PO_2, left ventricular puncture) were measured in pentobarbital-anesthetized mice. Lung mechanics were measured in identically treated mice using the flexivent system. Quasi-static compliance reflects the static elastic recoil pressure of the lungs at a given lung volume; Newtonian resistance represents the resistance of the central airways; dynamic resistance is a measure of the level of constriction in the lungs; dynamic elastance is a measure of the elastic rigidity of the lungs; intertance reflects the inertive properties of the gases in the airways; tissue damping reflects the energy dissipation in the lung tissues; tissue elastance is a measure of energy conservation in lung tissues; tissue hysteresivity is a measure of the ratio of energy dissipation to energy conservation in the lung tissue and the area of the pressure volume (PV) loop is an estimate of airspace closure before the PV curve maneuver (see http://www.scireq.com/science/measurements/).

mechanics in control mice and those with knockdown of the α3 laminin subunit using a flexiVent ventilator (Table 1). Pressure volume curves of the lungs were similar in both groups of mice, as were the main measures of lung compliance (Fig. 3A; Table 1). However, there was a reduction in the Newtonian resistance (a measure of central airways resistance) and an increase in hysteresivity in the α3-laminin-knockdown animals compared with controls, which was statistically significant even after correction for multiple comparisons (Table 1). We observed no significant differences in lung histology between control and knockdown animals (Fig. 3B).

Knockdown of the α3 laminin subunit is associated with mild lung inflammation

Bronchoalveolar lavage (BAL) fluid from the mice with knockdown of α3 laminin subunit contained more inflammatory cells than that obtained from Ad-Null-treated mice. The increased number of inflammatory cells was not observed in wild-type mice treated 60 days earlier with Ad-Null or Ad-Cre (supplementary material Fig. S2A). As the increase in inflammatory cells was not evident on histological sections, we performed a dispase digestion of the lungs from mice treated 60 days earlier with Ad-Null or Ad-Cre. The α3-laminin-knockdown animals showed increased numbers of alveolar macrophages, interstitial macrophages and neutrophils (Fig. 4A). In alveolar macrophages isolated from the dispase-digested lung we observed increased levels of the macrophage activation marker CD86 (Fig. 4B). In alveolar macrophages isolated from BAL we observed increased expression of CD86, as well as the macrophage activation markers CD40 and major histocompatibility complex (MHC) class II molecules (Fig. 4C; supplementary material Fig. S2C). The levels of inflammatory cells in the blood were similar in the control and knockdown animals (supplementary material Fig. S3).

The increased number of inflammatory cells prompted us to measure the levels of proinflammatory cytokines in the BAL fluid. Compared with Ad-Null-treated mice, mice with a knockdown of the α3 laminin subunit had a small, but significant, increase in the BAL concentrations of tumor necrosis factor (TNF)-α and monocyte chemoattractant protein (MCP)-1 (also known as C-C motif chemokine 2, CCL2). The levels of interleukin (IL)-6, interferon (IFN)-γ and IL-12p70 were higher in the Cre-treated animals, but these differences were not significantly significant (Fig. 4D).

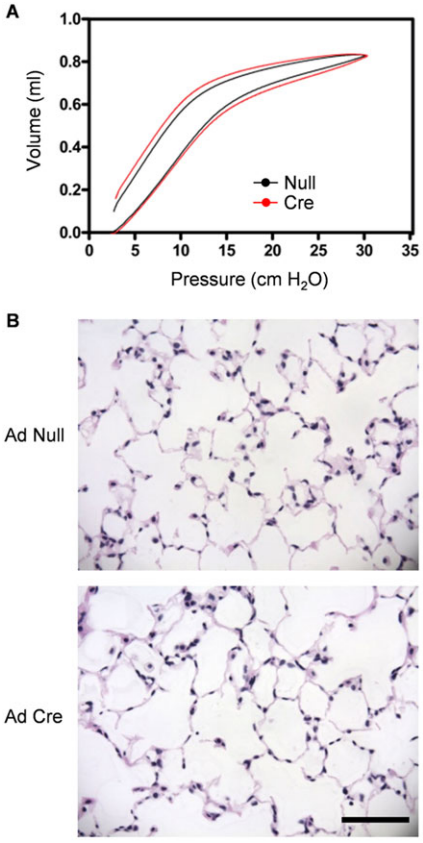

Fig. 3. The loss of the α3 laminin subunit in the adult lung is not associated with changes in lung mechanics or histological evidence of lung injury. (**A**) *Lama3*$^{fl/fl}$ mice were treated with a null adenovirus (Null) or an adenovirus encoding Cre recombinase (Cre); 60 days later lung mechanics, including pressure volume curves (A), were measured using the flexivent ventilator. Representative lung sections stained with hematoxylin and eosin are also shown (**B**). Scale bar: 25 μm.

Knockdown of the α3 laminin subunit protects against injurious ventilation

We exposed mice with knockdown of the α3 laminin subunit (treated with Ad-Cre 60 days earlier) and their controls (treated with Ad-Null 60 days earlier) to either non-injurious (12 ml per kg of body weight) or injurious (35 ml per kg of body weight) mechanical ventilation and measured several markers of the severity of lung injury (Fig. 5). Non-injurious mechanical ventilation of the α3-laminin-knockdown and control animals did not result in a significant change in lung compliance over the 120 minutes of the experiment. Control animals exposed to injurious mechanical ventilation demonstrated a progressive reduction in lung compliance over the duration of the mechanical ventilation. This reduction was attenuated in the mice with knockdown of the α3 laminin subunit (Fig. 5A). Because exposure to injurious mechanical ventilation resulted in the death of some animals, we compared the mortality during mechanical ventilation in mice with knockdown of the α3 laminin subunit with their controls. Injurious mechanical ventilation resulted in a significantly higher mortality in the control mice compared with the knockdown mice, whereas non-injurious ventilation was not associated with mortality in either group (Fig. 5B).

To determine whether the improved compliance observed in the α3-laminin-knockdown mice exposed to injurious mechanical ventilation was associated with an attenuation of lung injury, we compared histology and alveolar-capillary permeability in knockdown animals and their controls after 1 hour of exposure to injurious mechanical ventilation. This timepoint was chosen as it preceded the ventilator-associated mortality in both groups. Examination of lung sections stained with hematoxylin and eosin revealed less interstitial edema and hemorrhage in the knockdown animals compared with that in the controls (Fig. 5C). Similarly, the concentration of protein in the BAL fluid (a measure of the permeability of alveolar–capillary barrier) was lower in the knockdown animals compared with controls (Fig. 5D).

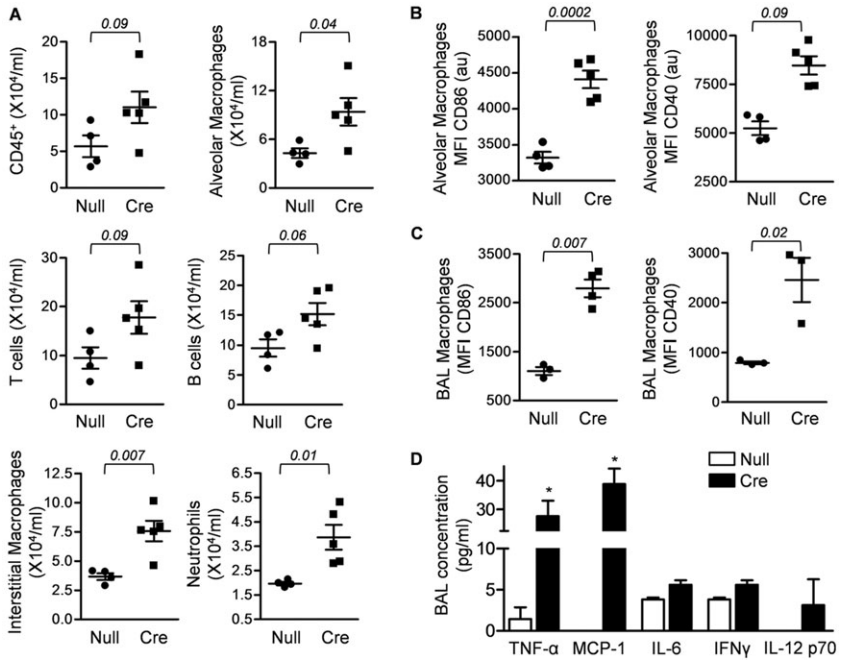

Fig. 4. The loss of the α3 laminin subunit in the adult lung leads to mild lung inflammation. *Lama3*$^{fl/fl}$ mice were treated with a null adenovirus (Null) or an adenovirus encoding Cre recombinase (Cre); 60 days later the lungs were digested with dispase and the cells were examined using flow cytometry. (**A**) Quantification of total (CD45^{+}) myeloid cells and specific inflammatory cells in the digested lung (see supplementary material Table S1 for specific markers). (**B**,**C**) Expression of the activation markers CD86 and CD40 on alveolar macrophages isolated from the dispase digested lung (B) and the BAL fluid (C). (**D**) BAL fluid levels of the proinflammatory cytokines, TNF-α, MCP-1, IL-6, IFNγ and IL12p70. Numerical values represent the *P*-value for comparison between Null and Cre. **P*<0.05 for comparison between Null and Cre.

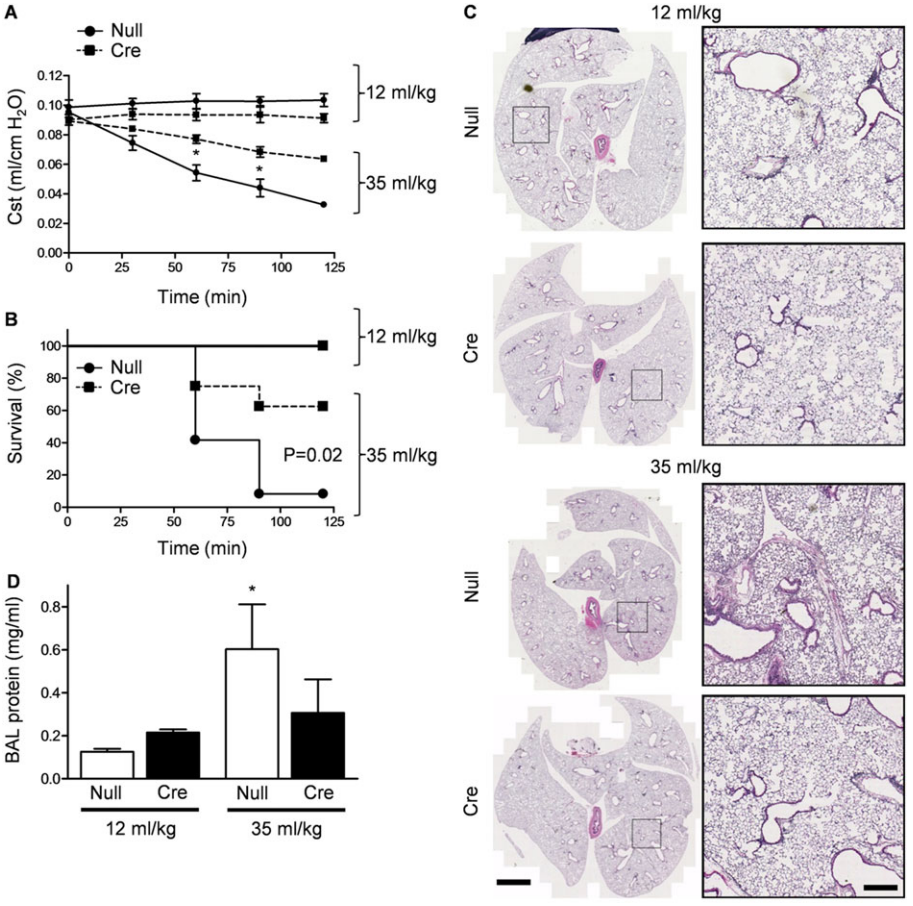

Fig. 5. The loss of the α3 laminin subunit in the adult lung confers resistance to mechanical ventilation induced lung injury. *Lama3*$^{fl/fl}$ mice were treated with a null adenovirus (Null) or an adenovirus encoding Cre recombinase (Cre) and 60 days later were subjected to 2 hours of non-injurious (tidal volume of 12 ml per kg of body weight) or injurious (tidal volume of 35 ml per kg of body weight) mechanical ventilation using a flexivent ventilator [minute ventilation matched, positive end-expiratory pressure (PEEP)=0]. Quasi-static lung compliance (**A**) and survival (**B**) were assessed every 30 minutes during the mechanical ventilation. After 1 hour of exposure, the lungs were harvested and composite sections stained with hematoxylin and eosin were examined at 100× magnification (**C**) (representative sections are shown). Alveolar capillary permeability to macromolecules was assessed by measuring total lung protein after 1 hour of mechanical ventilation (**D**). In A for 12 ml/kg n=4 for both Null and Cre groups; for 35 ml/kg, n=14 (Cre) and n=12 (Null). In the 35 ml/kg group, death of the animals [11 of 12 Null, 6 of 14 Cre, plotted in B] results in smaller sample sizes at the later time points. **P*<0.05 for comparison between Lama3 knockdown and control mice. Scale bars: 1 mm (C, left-hand panel) and 140 μm (C, right-hand panel).

Inflammation is not responsible for the resistance of the α3 laminin subunit knockdown animals to injurious ventilation

Surprisingly, we found that the increase in BAL cell count following injurious mechanical ventilation was markedly higher in the α3-laminin-knockdown animals compared with controls (Fig. 6A). To determine whether the low levels of TNF-α in the α3-laminin-knockdown mice protected against mechanical ventilation induced lung injury, we administered etanercept, a fusion protein containing the soluble TNF-α receptor 2 with the Fc portion of human IgG1, to mice 72 hours and 16 hours (300 μg per dose) before exposure to injurious mechanical ventilation (Trakala et al., 2009). Treatment with etanercept completely prevented the relative increase in BAL fluid cell count observed in the mice with knockdown of the α3 laminin subunit (Fig. 6A). Nevertheless, knockdown mice treated with etanercept showed a similar resistance to injurious ventilation to that of untreated mice. No protection against lung injury was observed in control (Ad-Null-treated) mice identically treated with etanercept (Fig. 6B; low volume ventilation controls are in supplementary material Fig. S4).

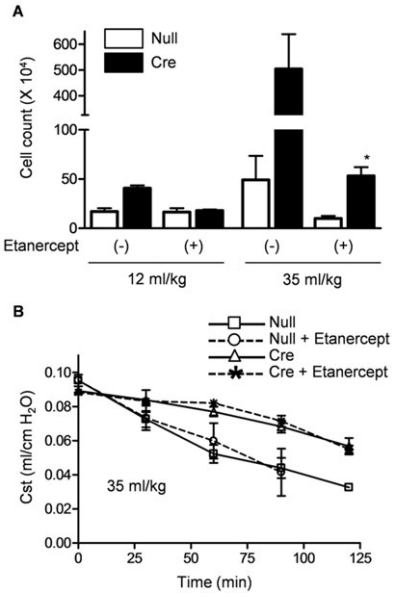

Fig. 6. TNF-α signaling is not responsible for the protection against mechanical-ventilation-induced lung injury conferred by the loss of the α3 laminin subunit. *Lama3*$^{fl/fl}$ mice were treated with a null adenovirus (Null) or an adenovirus encoding Cre recombinase (Cre) and 60 days later were subjected to 2 hours of non-injurious (tidal volume of 12 ml per kg of body weight; supplementary material Fig. S2) or injurious (tidal volume of 35 ml per kg of body weight) mechanical ventilation using a flexivent ventilator [minute ventilation matched, positive end-expiratory pressure (PEEP)=0]. BAL fluid levels of leukocytes were measured after 1 hour of ventilation (**A**). $P<0.05$ for comparison between etanercept- and vehicle-treated animals ($n>4$ for each group). In a separate group of identically treated mice, quasi-static lung compliance was measured every 30 minutes during mechanical ventilation (**B**). There was no significant difference between etanercept- and vehicle-treated animals; $P<0.05$ for comparison between Null- and Cre-treated animals ($n>6$ for each group).

Signaling pathways upon ventilation are unaffected by knockdown of the a3 laminin subunit

We have previously reported that interaction between the α3 laminin subunit and dystroglycan was required for the activation of signaling pathways, including the ERK1/2 pathway, induced by mechanical stretch in the lung (Jones et al., 2005). As ERK1/2 and other signaling pathways have been reported to regulate the response to injurious ventilation, we reasoned that the loss of the α3 laminin subunit might confer a resistance to mechanical ventilation induced lung injury by inhibiting the activation of injurious signaling pathways in the lung. To test this hypothesis, we examined the activation of several signaling pathways previously reported to modulate the severity of acute lung injury in whole lung homogenates from mice treated with injurious (35 ml per kg of body weight) ventilation for 20 minutes (Dolinay et al., 2008; Le et al., 2008; Villar et al., 2010). Injurious ventilation induced a similar activation of the ERK1/2 and JNK pathways in both control mice and upon knockdown of the α3 laminin subunit (Fig. 7A,B). No degradation of IκBα (Fig. 7C) or activation of p38 MAPK (supplementary material Fig. S5) was observed following mechanical ventilation in either control mice or those with α3 laminin subunit knockdown.

Collagen I deposition is promoted in the lung following knockdown of the α3 laminin subunit

Hayashida et al. reported that the loss of interactions between laminin and epithelial integrins can promote tissue fibrosis, which might explain the resistance to mechanical injury observed in the α3-laminin-knockdown animals (Hayashida et al., 2010). We found a significant increase in total lung collagen levels in the α3-laminin-knockdown animals when compared with control-treated animals using Picrosirius Red collagen precipitation (Fig. 8A). Immunoblotting of total lung homogenates using antibodies that recognize type I and type IV collagen, revealed a significant increase in type I collagen (Fig. 8B) but no change in type IV collagen (supplementary material Fig. S4) in the lungs of the animals with α3 laminin subunit knockdown. We also used second-harmonic wave generation to image collagen deposition in unstained 5-μm lung sections. In the α3-laminin-knockdown animals, we observed increased staining for collagen throughout the lung parenchyma (Fig. 8C). We measured fluorescence intensity as a method to provide a relative quantification (Fig. 8C). These results were confirmed by examining Sirius-Red-stained lung sections using polarized light (Fig. 8D).

Discussion

Although it is known that the timed expression of specific laminin isoforms is required for normal lung development, the role played by laminins in the adult lung is not well understood (Nguyen et al., 2005). The α3 laminin subunit is abundantly expressed in the adult lung, either as part of laminin 311 or 332 (DeBiase et al., 2006; Jones et al., 2005; Miner, 2008; Nguyen et al., 2005; Nguyen and Senior, 2006; Pierce et al., 2000; Pierce et al., 1998). These laminins are localized in the basement membrane of the airway and the specialized alveolar–capillary basement membrane of the lung (Miner, 2008; Pierce et al., 2000). This basement membrane links the flattened alveolar epithelial cells and endothelial cells, which together create a nearly two-dimensional structure that offers little resistance to gas exchange (Weibel, 1963). The viscoelastic properties of these

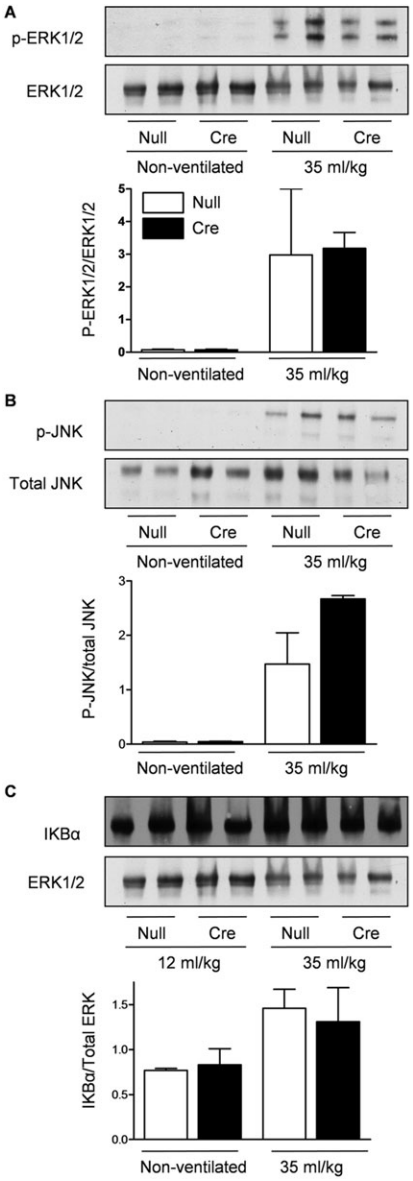

Fig. 7. The loss of the α3 laminin subunit in the adult lung does not prevent the activation of MAPK pathways in the lung. *Lama3*$^{fl/fl}$ mice were treated with a null adenovirus (Null) or an adenovirus encoding Cre recombinase (Cre) and 60 days later were untreated or subjected to injurious (tidal volume of 35 ml per kg of body weight) mechanical ventilation using a flexivent ventilator [minute ventilation matched, positive end-expiratory pressure (PEEP)=0]. After 20 minutes, lung homogenates were immunoblotted using antibodies against (**A**) phosphorylated ERK1/2 (p-ERK1/2) and total ERK1/2, (**B**) phosphorylated JNK (p-JNK) and total JNK and (**C**) IκBα. No significant difference in the activation of these signaling pathways between Null- and Cre-treated animals was detected. Representative blots are shown. A minimum of four animals per group were assayed. The results for phosphorylated and total MAPK p38 are shown in supplementary material Fig. S5.

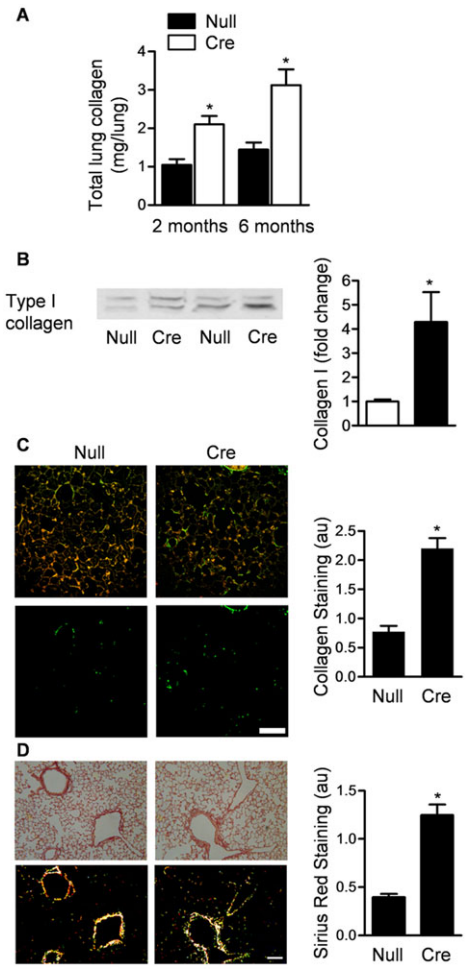

Fig. 8. The loss of the α3 laminin subunit in the adult lung is associated with an increase in collagen I. (**A**) *Lama3*$^{fl/fl}$ mice were treated with a null adenovirus (Null) or an adenovirus encoding Cre recombinase (Cre) and 60 days or 6 months later lung homogenates were analyzed for total collagen using picrosirius red collagen precipitation ($n>7$ per group). (**B**) The levels of collagen I were measured in lung homogenates by immunoblotting using a collagen I polyclonal antiserum, representative blots of those from four animals are shown, densitometry analysis are on the right-hand side. (**C**) Unstained lung sections (5 μm) from mice treated with Null or Cre 60 days earlier were examined for collagen staining using second-harmonic wave generation. Collagen is shown in the bottom panels; a quantification is shown on the right-hand side. (**D**) Sirius-Red-stained lung sections from mice treated with Null or Cre 60 days earlier were examined for collagen staining using polarized light (bottom panels); a quantification is shown on the right-hand side ($n=3$ for C and D). *$P<0.05$ for comparison between Null and Cre.

alveolar capillary units contribute to the normal mechanics of the lung, which allows the efficient exchange between the blood and the ambient air. In this study, we generated a mouse harboring a conditional knockout of the α3 laminin subunit, a component of both of the main laminin isoforms in the lung. The lung-specific delivery of Cre recombinase using an adenoviral vector resulted in a progressive and specific knockdown of α3 laminin over a period of 60 days. The expression of adenovirally delivered Cre recombinase is maximal within 48 hours after infection and genetic recombination occurs rapidly (Branda and Dymecki, 2004; Rosenfeld et al., 1992). We can therefore infer from these experiments that laminin in the basement membrane has a remarkably long half-life (between 30 and 60 days), providing direct evidence that laminins, and perhaps other basement membrane proteins, turn over slowly in the adult lung.

Global knockout of the α3 laminin subunit in mice results in severe skin blistering and the death of the animals shortly after birth (Ryan et al., 1999). Consistent with these findings,

mutations in the human *LAMA3* gene have been identified in patients with junctional epidermolysis bullosa, a blistering skin disease characterized by a separation between the dermal and epidermal layers of the skin in response to minor trauma (Laimer et al., 2010). We reasoned that the loss of the α3 laminin subunit in the lung might worsen the response of the lung to mechanical trauma in the form of positive pressure ventilation. Surprisingly, we observed that mice with a knockdown of the α3 laminin subunit in the lung were protected against the reduction in compliance associated with injurious mechanical ventilation. Compared with control mice, knockdown mice had decreased evidence of lung injury histologically and exhibited a smaller increase in the permeability of the alveolar–capillary barrier to macromolecules. These results are consistent with the lack of reports of a pulmonary phenotype in infants with junctional epidermolysis bullosa, many of whom require mechanical ventilation as part of their supportive care (Laimer et al., 2010).

Surprisingly, we found that the number of inflammatory cells was increased in the lung both at baseline and with mechanical ventilation in the animals with knockdown of the α3 laminin subunit. Alveolar macrophages from the α3-laminin-knockdown animals expressed higher levels of activation markers on their surface at baseline, and BAL fluid levels of proinflammatory cytokines in the alveolar space were higher at baseline and after injurious ventilation in the α3-laminin-knockdown animals. This was not a direct effect of the adenoviral infection as neither wild-type animals treated with the Cre virus nor the *Lama3*$^{fl/fl}$ mice treated with a null virus exhibited similar abnormalities. Although the reason for this inflammation is not clear, Adair-Kirk et al. have reported that a peptide motif present in the α5 but not α3 subunit of laminin was sufficient to induce chemotaxis and the production of matrix metalloproteinase-9 when applied to murine macrophages or administered intranasally into the lungs of mice (Adair-Kirk et al., 2003). Although we did not observe a compensatory increase in α5 laminin upon knockdown of the α3 laminin subunit, these results, taken together with our findings, suggest that laminins play an important role in modulating the inflammatory response in the lung.

There was a significant increase in TNF-α in the BAL of the *Lama3*$^{fl/fl}$ mice treated with Cre virus. Although the increased levels of TNF-α before exposure to injurious mechanical ventilation that we have observed would be predicted to worsen ventilator-induced lung injury, pretreatment with a low dose of TNF-α has been shown to attenuate injury in other models (Imai et al., 1999; Nawashiro et al., 1997). Although pre-treatment of animals exhibiting α3 laminin subunit lung deficiency with etanercept, a potent inhibitor of TNF-α, prevented the basal and mechanical ventilation-induced increases in the BAL lymphocytes, treatment with etanercept did not alter the severity of mechanical-ventilation-induced injury in either the wild-type mice or those with α3 laminin subunit knockdown. Although it remains possible that the low levels of inflammation observed after the loss of α3 laminin contributed to the development of fibrosis, this would appear unlikely given that our group and others have reported that lung inflammation is insufficient to induce lung fibrosis (Budinger et al., 2006; Munger et al., 1999).

We propose that the resistance to mechanical-ventilation-induced lung injury in the α3-laminin-knockdown mice was attributable to a homogenous increase in collagen I in the connective tissue compartment of the lung that followed the loss of the α3 laminin subunit. This increase in collagen might have resulted from the loss of interactions between laminins and epithelial or endothelial surface proteins that inhibit profibrotic pathways. For example, it is known that the activation of the profibrotic cytokine TGF-β1 requires increased expression of the integrin αvβ6 (Munger et al., 1999). In this regard, it has been reported that sequestration of β1 integrins by laminins in endothelial cells inhibited the ligand binding of αv-containing integrins (Gonzalez et al., 2002). Thus it is possible that the upregulation of collagen I expression in α3-laminin-deficient lungs is a consequence of activation of αvβ6 integrin due to a release of the inhibitory effects of laminin-binding integrins. Such a model would be consistent with recent data indicating that loss of integrin signaling was sufficient to activate TGF-β1 signaling and increase the expression of collagen I in kidney epithelial cells (Hayashida et al., 2010).

We delivered Cre recombinase to the lungs of mice by administering a high dose of a replication-deficient adenoviral vector in a surfactant vehicle, as described previously (Mutlu et al., 2004). Adenoviruses preferentially infect cells expressing the Cocksakie A receptor (CAR), a junctional adhesion molecule (JAM) localized to tight junctions in the airway and alveolar epithelium (Cohen et al., 2001). Following infection with adenoviruses, expression of the transgene is maximal after 48 hours and is not detectable after 10 days (Dumasius et al., 2003). Using β-galactosidase Cre reporter mice, we have previously shown that administration of adenoviral Cre at this dose results in widespread recombination in the airway and alveolar epithelium (Budinger et al., 2010; Weinberg et al., 2010). At 60 days after infection with adenoviral Cre, we found that α3 laminin was knocked down in alveolar type II cells, collagen deposition was increased in the alveolar space and activation markers were expressed on the surface of alveolar macrophages. These results suggest that collagen deposition and inflammation are increased in the alveolar compartment in the α3-laminin-knockdown animals. It remains possible, however, that knockdown of α3 laminin in the airways, or other cell types within the lung, might have contributed to the observed phenotype. In addition, although wild-type mice infected with an adenovirus develop inflammation that is maximal 2 days after the infection and is undetectable after 10 days, we cannot exclude the possibility that the inflammation and collagen deposition we observed in the lungs upon α3 laminin knockdown at 60 days after infection results from impaired resolution of virally induced lung injury (Dumasius et al., 2003).

In summary, we have demonstrated that the α3 laminin subunit has a long half-life in the adult lung and that knockdown of this protein in the lung is associated with an increase in the abundance of type I collagen in the alveolar basement membrane. We speculate that this increase in collagen confers a resistance to mechanical-ventilation-induced lung injury. Although lung inflammation appeared to be enhanced in the animals with knockdown of the α3 laminin subunit, this did not explain the observed protection against injurious ventilation. Rather, our results strongly suggest that the loss of an interaction between laminins containing the α3 subunit in the lung and proteins in the alveolar epithelium or endothelium is permissive for the development of lung fibrosis.

Materials and Methods

Generation of Lama3 floxed mice and alveolar type II cell isolation

All experiments using mice were approved by the Animal Care and Use Committee at Northwestern University. We generated an inducible knockout mouse using a vector targeting exon 42 of the mouse *Lama3* gene (the murine

equivalent of human exon 41 of *LAMA3*) by positioning *loxP* sequences 3 kb upstream and 4 kb downstream of exon 42 according to a method that has been previously described (Koentgen et al., 2010). For all experiments, we used mice that were 6–8 weeks of age (20–25 g). All mice are on a C57BL/6 background. Wild-type control mice were purchased from Jackson Laboratories. Primer sequences for PCR on lung genomic DNA are given in supplementary material Table S4. Alveolar type II cells were isolated from mouse lungs as previously described (Budinger et al., 2006).

Adenoviral infection of mice

High-titer ($>10^{12}$ pfu per ml) first-generation adenoviral vectors encoding Cre recombinase (Ad-Cre) or no transgene (Ad-Null) were purchased from Viraquest (Liberty City, Iowa). Viraquest provided viral titers and excluded wild-type viral contamination of the viral vectors (negative PCR for glycoprotein E1). Mice were infected with adenoviral vectors (1×10^9 pfu per animal) in 50% surfactant vehicle, balanced with TE buffer as previously described (Mutlu et al., 2004). The mice were housed in a barrier facility in microisolator cages for up to 60 days after the adenoviral infection.

Antibodies

To generate an antiserum that detects mouse α3 laminin, we first prepared a bacterial expression vector, pSTBLUE-1, containing sequence encoding the G1–G2 domains of the murine α3 laminin subunit. This construct was transfected into *Escherichia coli* and expression of the protein fragment was induced following treatment wiith 1 mM isopropyl β-D-thiogalactopyranoside, according to the manufacturer's recommendations (Novagen EMD Chemicals). The protein was partially purified using column chromatography and then processed for SDS-PAGE. Recombinant protein was visualized on gels following staining with Coomassie Brilliant Blue. The stained protein bands were excised from gels, frozen and sent to EZBiolab (Carmel, IN) for rabbit antiserum generation. Specificity of the antiserum was confirmed by immunoblotting using laminin 332 matrix derived from mouse keratinocytes.

A mouse monoclonal antibody against the α3 laminin subunit (10B5) was described previously (Goldfinger et al., 1999). A goat polyclonal antibody against collagen I was obtained from Southern Biotech (Birmingham, AL). An antibody against the γ1 laminin subunit was purchased from Santa Cruz Biotechnology (Santa Cruz, CA). Antibodies against the β1 and α5 laminin subunits were generous gifts of Peter Yurchenco, Robert Wood Johnson University Hospital, Piscataway, NJ and Jeffrey Miner, Washington University, St Louis, MO, respectively. Antibodies against phosphorylated ERK1/2, total ERK1/2, phosphorylated JNK, total JNK, pan-phosphorylated p38 MAPK, pan-total p38 MAPK, lamin A/C and IκBα were obtained from Cell Signaling Technology (Danvers, MA). Secondary antibodies conjugated with various fluorochromes or horseradish peroxidase were purchased from Jackson ImmunoResearch Laboratories. Antibodies used for flow cytometry are detailed in supplementary material Table S1.

Tissue staining and analysis

A 20-gauge Angiocath was sutured into the trachea, the lungs and heart were removed en bloc, and the lungs were inflated to 20 cm H_2O with 4% paraformaldehyde. The heart and lungs were fixed in paraffin, and 5-μm sections were stained with hematoxylin and eosin and Masson's Trichrome stain (for detection of collagen fibers) (Budinger et al., 2006). Low-power field images of whole mouse lungs (50×) were obtained using Neurolucida Software (MBF Biosciences, Williston, VT). For immunofluorescence analyses, lung tissue was rapidly frozen in Tissue-Tek OCT compound (Electron Microscopy Sciences, Hatfield, PA) and 8-μm sections were prepared on a cryo-microtome. Frozen sections were mounted onto microscope slides, fixed for 2 minutes in –20℃ acetone, air dried and then incubated for 2 hours at room temperature with antibody against either the mouse α3 laminin subunit or collagen I, diluted in PBS. The sections were then washed extensively and subsequently incubated for 1 hour at 37℃ in rhodamine-conjugated secondary antibody. After further washing, the sections were covered with mounting medium and a coverslip. Images of the stained lung sections were captured using a Zeiss LSM 510 META laser scanning confocal microscope and exported to ImageJ (NIH, Bethesda, MD) where line-scan plot profiles were analyzed across the areas shown. This analysis generates plots indicating changes in the relative fluorescence intensities across arbitrary regions of the imaged specimen.

SDS-PAGE and immunoblotting

Terminally anesthetized mice underwent laparotomy and a left nephrectomy. The thorax was then opened medially, the right ventricle was cannulated and perfused with ~1 ml of sterile PBS (until the lungs cleared of blood). The lungs were then removed at the hila, placed in sample buffer (10 mM Tris-HCl pH 6.8, 8 M urea, 1% SDS and 15% β-mercaptoethanol) and homogenized using a tissue homogenizer (for 10 seconds on ice) (Laemmli, 1970). Proteins were separated by SDS-PAGE, transferred onto nitrocellulose and processed for immunoblotting as previously described (Klatte et al., 1989; Laemmli, 1970). Immunoblots from a minimum of three separate assays were scanned and quantified using Molecular Analyst (Bio-Rad). Examination of phosphorylated proteins in lung homogenates was performed in an identical manner, except that a modified RIPA buffer was used for tissue lysis. To evaluate the relative levels of phosphorylation of a target protein in a test sample, protein preparations were subjected to SDS-PAGE on two identical gels, and the proteins were transferred onto two separate pieces of nitrocellulose. One of the pieces of nitrocellulose was probed with antibody against the phosphorylated form of the protein, and the other was processed with antibody that recognizes the same protein regardless of its phosphorylation state. The level of phosphorylation of an assayed protein was calculated relative to the total amount of the same protein in each sample. We then calculated the difference in phosphorylation of the test protein in each sample relative to that observed in the control. To assess collagen 1 levels by immunoblotting, acetic acid extracts of lung tissue (see below) were diluted into SDS-PAGE sample buffer and the solution neutralized. The protein preparation was subjected to SDS-PAGE and transferred onto nitrocellulose. The latter was processed with antibody as above.

Measurement of total lung collagen

Lung collagen was measured using a modification of a previously described method for the precipitation of lung collagen using Picrosirius Red (Whittaker et al., 1994). Mouse lungs were harvested and suspended in 0.5 M acetic acid and then homogenized, first with a tissue homogenizer (60 seconds on ice) and then using 20 strokes in a Dounce homogenizer (on ice). The resulting homogenate was spun (10,000 ***g***) for 10 minutes and the supernatant was used for subsequent analyses. A portion of this supernatant was also processed for immunoblotting (see above). Collagen standards were prepared in 0.5 M acetic acid using rat-tail collagen (Sigma-Aldrich). Picrosirius Red dye was prepared by mixing 0.2 g of Sirius Red F3B (Sigma-Aldrich) with 200 ml of water; 1 ml of the Picrosirius Red dye was added to 50 μl of the collagen standard or the lung homogenates and then mixed continuously at room temperature on an orbital shaker for 30 minutes. The precipitated collagen was then pelleted and washed once with 0.5 M acetic acid (10,000 ***g*** for 10 minutes each). The resulting pellet was resuspended in 500 μl of 0.5 M NaOH and Sirius Red staining was quantified spectrophotometrically (540 nm) using a colorimetric plate reader (Bio-Rad).

Bronchoalveolar lavage (BAL) fluid analysis

BAL was performed through a 20-gauge Angiocath ligated into the trachea (Mutlu et al., 2004). A 1.0-ml aliquot of PBS was instilled into the lungs and then carefully aspirated three times. A 100-μl aliquot of the BAL fluid was placed in a cytospin and centrifuged at 500 ***g*** for 5 minutes. For cytokine measurement, the BAL fluid was centrifuged at 200 ***g*** for 10 minutes, and the supernatant was used for the measurement of BAL protein (Bradford) and proinflammatory cytokine levels using the BD Bioscience cytometric bead array mouse inflammation kit, which detects IL-6, -10, and 2, MCP-1, IFN-γ and TNF-α, according to the instructions provided.

Exposure to injurious mechanical ventilation and measurement of lung mechanics and gas exchange

Exposure to mechanical ventilation and measurements of lung mechanics were performed using a flexiVent mouse ventilator (Scireq, Montreal, Canada) according the protocols established by Scireq (Vanoirbeek et al., 2010). A standard ventilation history for each mouse was obtained with two total lung capacity (TLC) maneuvers before the forced oscillation and quasi-static pressure volume curve protocols that were used to calculate airway resistance, inertance, tissue damping, tissue elastance and quasi-static lung compliance. Arterial blood gas analysis was performed in pentobarbital sedated nonventilated animals using a Stat Profile pHOx blood gas analyzer (Nova Biomedical).

Flow cytometry

For BAL fluid and lung digests, the aortas of terminally sedated mice were cut and the right ventricle was perfused with PBS to remove blood from the lungs. A tracheostomy tube was placed before removal of the heart and lungs en bloc. The lungs were filled with 0.8 ml dispase (BD Bioscience) at room temperature and placed in a 50-ml Falcon tube with 0.8 ml dispase on an orbital shaker (45 minutes, room temperature). The lungs were then placed in a 10 cm^2 dish with 0.04 mg/ml DNase Type II-S lyophilized powder (0.04 mg/ml, Sigma-Aldrich, in DMEM) and the tissue was teased apart using curved forceps. The tissue was then strained through a 70-μm filter using 2 ml DMEM and stored on ice before flow cytometry. Before flow cytometry, red blood cells were lysed using the BD Pharm Lyse lysing buffer (BD Biosciences) and were counted using a Countess cell counter (Invitrogen). For flow cytometric analysis, 2×10^6 cells were blocked with Mouse BD FcBlock (BD Biosciences) and stained with a cocktail of fluorochrome-conjugated antibodies (supplementary material Table S1). Samples were acquired on BD LSR II instrument (the instrument configuration, including lasers, mirrors and filters, is provided in supplementary material Table S2). At least 100,000 events in the $CD45^+$ gate were acquired. Data were analyzed using

FlowJo 9.2 software; sequential gating was used to avoid overlap between populations. Absolute cell counts for specific cell populations were calculated by multiplying the total number of cells obtained by using the cell counter by the percentages obtained by flow cytometry. Population definitions are described in supplementary material Table S3.

Blood was obtained by cardiac puncture of the deeply anesthetized mouse. Sodium citrate was used as an anticoagulant. Staining for flow cytometry was performed within 2 hours after the harvesting. A total of 50 µl of citrated blood were incubated with Mouse BD FcBlock (BD Biosciences) for 10 minutes at 4℃ and then stained with a cocktail of fluorochrome-conjugated antibodies for 30 minutes at 4℃ (see supplementary material Table S1 for details on antibodies) in a total volume of 100 µl. Fixation and red blood cell lysis was performed using 1 ml of BD FACS lysing solution (BD Biosciences). Cells were washed twice with the FACS buffer (2% fetal calf serum in PBS), and images were acquired on the BD LSR II instrument (see supplementary material Table S2 for details on instrument configuration). At least 50,000 events in the $CD45^+$ gate were collected for analysis. The total white blood cell count was obtained using a Hemavet 950 analyzer.

Assessment of lung collagen using Picrosirius Red staining and second-harmonic wave generation

Images for collagen accumulation were acquired using two methods. Paraffin-embedded lung tissue from two untreated, three null- and three Cre-treated *Lama3* floxed mice were cut into two sets of 5-µm thick slices. The first set was processed and stained with Picrosirius Red dye, and images were captured for each sample using a 10× objective (0.25 N.A.) on a Leitz Dialux 20 microscope equipped with an Olympus DP72 cooled digital color camera and a circularly polarized light filter to visualize collagen. CellSens Entry 1.3 software was used to collect the images, which were further processed and quantified using ImageJ 1.38x software. Masks of the total alveolar area were created from the bright-field images and were then overlaid onto the similarly thresholded polarized images to determine the percentage of alveolar area (in pixels) containing collagen for each field of view. These areas were averaged from at least 10 images per mouse.

Unstained tissue slices from the same mice were also imaged using a 10× water objective (0.3 N.A.) on an Olympus Fluoview FV1000MPE Basic multiphoton laser scanning microscope. A 860-nm pulsed laser was used for excitation, and emitted light was collected through a filter containing a 485 nm dichroic mirror and two band pass filters: 495–540 nm for tissue autofluorescence and 420–460 nm for second-harmonic wave generation to visualize collagen. The images were collected using the Olympus FV10-ASW software and then processed using Photoshop and ImageJ. Images of the tissue autofluorescence were used to create total alveolar area masks, which were then overlaid onto the second-harmonic wave signal to determine the percentage of alveolar area (in pixels) containing collagen for each field of view. These areas were averaged from at least seven images per mouse.

Quantitative real-time PCR (qRT-PCR) measurement of RNA

We isolated total RNA using a commercially available system (TRIzol, Invitrogen) from mouse lungs (Bustin et al., 2009; Pfaffl, 2001) and performed qRT-PCR reactions using IQ SYBR Green superscript with the primers listed in supplementary material Table S4, analyzed on a Bio-Rad IQ5 real-time PCR detection system. We employed the Pfaffl method to analyze the normalized data as previously described (Bustin et al., 2009; Pfaffl, 2001).

Statistics

Differences between groups were explored using ANOVA. When the ANOVA indicated a significant difference, individual differences were explored using Student's *t*-tests with a Dunnett or Bonferonni correction for multiple comparisons. Mortality differences were determined using a Kaplan–Meier analysis. All analyses were performed using GraphPad Prism version 4.00 for Windows (GraphPad Software, San Diego California). Data are shown as means ± s.e.m.

This work was supported by NIH HL092963 (G.R.S.B., J.C.R.J.), ES015024 (G.M.M.), American Lung Association (G.M.M.), NIH ES013995 (G.R.S.B.), NIH HL071643 (G.M.M., G.R.S.B.), Northwestern University Clinical and Translational Sciences Institute (NUCATS) CTI Pilot Award (UL1 RR025741; NCCR), (G.M.M.), NIH AR050250 (H.P.), NIH AR054796 (H.P.), NIH AR055503 (H.P.) and NIH AI067590 (H.P.) and funds provided by Northwestern University, Feinberg School of Medicine (H.P.). Deposited in PMC for release after 12 months.

Supplementary material available online at
http://jcs.biologists.org/lookup/suppl/doi:10.1242/jcs.080911/-/DC1

References

Adair-Kirk, T. L., Atkinson, J. J., Broekelmann, T. J., Doi, M., Tryggvason, K., Miner, J. H., Mecham, R. P. and Senior, R. M. (2003). A site on laminin {alpha}5, AQARSAASKVKVSMKF, induces inflammatory cell production of matrix metalloproteinase-9 and chemotaxis. *J. Immunol.* **171**, 398-406.

Branda, C. S. and Dymecki, S. M. (2004). Talking about a revolution: the impact of site-specific recombinases on genetic analyses in mice. *Dev. Cell* **6**, 7-28.

Budinger, G. R., Mutlu, G. M., Eisenbart, J., Fuller, A. C., Bellmeyer, A. A., Baker, C. M., Wilson, M., Ridge, K., Barrett, T. A., Lee, V. Y. et al. (2006). Proapoptotic bid is required for pulmonary fibrosis. *Proc. Natl. Acad. Sci. USA* **103**, 4604-4609.

Budinger, G. R. S., Urich, D., DeBiase, P. J., Chiarella, S. E., Burgess, Z. O., Baker, C. M., Soberanes, S., Mutlu, G. M. and Jones, J. C. R. (2008). Stretch-induced activation of AMP kinase in the lung requires dystroglycan. *Am. J. Respir. Cell Mol. Biol.* **39**, 666-672.

Budinger, G. R. S., Mutlu, G. M., Urich, D., Soberanes, S., Buccellato, L. J., Hawkins, K., Chiarella, S. E., Radigan, K. A., Eisenbart, J., Agrawal, H. et al. (2010). Epithelial cell death is an important contributor to oxidant-mediated acute lung injury. *Am. J. Respir. Crit. Care Med.* **183**, 1043-1054.

Bustin, S. A., Benes, V., Garson, J. A., Hellemans, J., Huggett, J., Kubista, M., Mueller, R., Nolan, T., Pfaffl, M. W., Shipley, G. L. et al. (2009). The MIQE guidelines: minimum information for publication of quantitative real-time PCR experiments. *Clin. Chem.* **55**, 611-622.

Cohen, C. J., Shieh, J. T., Pickles, R. J., Okegawa, T., Hsieh, J. T. and Bergelson, J. M. (2001). The coxsackievirus and adenovirus receptor is a transmembrane component of the tight junction. *Proc. Natl. Acad. Sci. USA* **98**, 15191-15196.

DeBiase, P. J., Lane, K., Budinger, S., Ridge, K., Wilson, M. and Jones, J. C. R. (2006). Laminin-311 (Laminin-6) fiber assembly by type I-like alveolar cells. *J. Histochem. Cytochem.* **54**, 665-672.

Dolinay, T., Wu, W., Kaminski, N., Ifedigbo, E., Kaynar, A. M., Szilasi, M., Watkins, S. C., Ryter, S. W., Hoetzel, A. and Choi, A. M. (2008). Mitogen-activated protein kinases regulate susceptibility to ventilator-induced lung injury. *PLoS ONE* **3**, e1601.

Dumasius, V., Jameel, M., Burhop, J., Meng, F. J., Welch, L. C., Mutlu, G. G. and Factor, P. (2003). In vivo timing of onset of transgene expression following adenoviral-mediated gene transfer. *Virology* **308**, 243-249.

Goldfinger, L. E., Hopkinson, S. B., deHart, G. W., Collawn, S., Couchman, J. R. and Jones, J. C. (1999). The alpha3 laminin subunit, alpha6beta4 and alpha3beta1 integrin coordinately regulate wound healing in cultured epithelial cells and in the skin. *J. Cell Sci.* **112**, 2615-2629.

Gonzalez, A. M., Gonzales, M., Herron, G. S., Nagavarapu, U., Hopkinson, S. B., Tsuruta, D. and Jones, J. C. R. (2002). Complex interactions between the laminin α4 subunit and integrins regulate endothelial cell behavior in vitro and angiogenesis in vivo. *Proc. Natl. Acad. Sci. USA* **99**, 16075-16080.

Hayashida, T., Jones, J. C. R., Lee, C. K. and Schnaper, H. W. (2010). Loss of β1-integrin enhances TGF-β1-induced collagen expression in epithelial cells via increased αvβ3-integrin and Rac1 activity. *J. Biol. Chem.* **285**, 30741-30751.

Imai, Y., Kawano, T., Iwamoto, S., Nakagawa, S., Takata, M. and Miyasaka, K. (1999). Intratracheal anti-tumor necrosis factor-alpha antibody attenuates ventilator-induced lung injury in rabbits. *J. Appl. Physiol.* **87**, 510-515.

Jones, J. C., Lane, K., Hopkinson, S. B., Lecuona, E., Geiger, R. C., Dean, D. A., Correa-Meyer, E., Gonzales, M., Campbell, K., Sznajder, J. I. et al. (2005). Laminin-6 assembles into multimolecular fibrillar complexes with perlecan and participates in mechanical-signal transduction via a dystroglycan-dependent, integrin-independent mechanism. *J. Cell Sci.* **118**, 2557-2566.

Klatte, D. H., Kurpakus, M. A., Grelling, K. A. and Jones, J. C. (1989). Immunochemical characterization of three components of the hemidesmosome and their expression in cultured epithelial cells. *J. Cell Biol.* **109**, 3377-3390.

Koentgen, F., Suess, G. and Naf, D. (2010). Engineering the mouse genome to model human disease for drug discovery. *Methods Mol. Biol.* **602**, 55-77.

Laemmli, U. K. (1970). Cleavage of structural proteins during the assembly of the head of bacteriophage T4. *Nature* **227**, 680-685.

Laimer, M., Lanschuetzer, C. M., Diem, A. and Bauer, J. W. (2010). Herlitz junctional epidermolysis bullosa. *Dermatol. Clin.* **28**, 55-60.

Le A., Damico, R., Damarla, M., Boueiz, A., Pae, H. H., Skirball, J., Hasan, E., Peng, X., Chesley, A., Crow, M. T. et al. (2008). Alveolar cell apoptosis is dependent on p38 MAP kinase-mediated activation of xanthine oxidoreductase in ventilator-induced lung injury. *J. Appl. Physiol.* **105**, 1282-1290.

Martin, G. R. and Timpl, R. (1987). Laminin and other basement membrane components. *Annu. Rev. Cell Biol.* **3**, 57-85.

Miner, J. H. (2008). Laminins and their roles in mammals. *Microsc. Res. Tech.* **71**, 349-356.

Munger, J. S., Huang, X., Kawakatsu, H., Griffiths, M. J., Dalton, S. L., Wu, J., Pittet, J. F., Kaminski, N., Garat, C., Matthay, M. A. et al. (1999). The integrin alpha v beta 6 binds and activates latent TGF beta 1, a mechanism for regulating pulmonary inflammation and fibrosis. *Cell* **96**, 319-328.

Mutlu, G. M., Dumasius, V., Burhop, J., McShane, P. J., Meng, F. J., Welch, L., Dumasius, A., Mohebahmadi, N., Thakuria, G., Hardiman, K. et al. (2004). Upregulation of alveolar epithelial active Na+ transport is dependent on beta2-adrenergic receptor signaling. *Circ. Res.* **94**, 1091-1100.

Nawashiro, H., Tasaki, K., Ruetzler, C. A. and Hallenbeck, J. M. (1997). TNF-[alpha] pretreatment induces protective effects against focal cerebral ischemia in mice. *J. Cereb. Blood Flow Metab.* **17**, 483-490.

Nguyen, N. M. and Senior, R. M. (2006). Laminin isoforms and lung development: all isoforms are not equal. *Dev. Biol.* **294**, 271-279.

Nguyen, N. M., Kelley, D. G., Schlueter, J. A., Meyer, M. J., Senior, R. M. and Miner, J. H. (2005). Epithelial laminin [alpha]5 is necessary for distal epithelial cell maturation, VEGF production, and alveolization in the developing murine lung. *Dev. Biol.* **282**, 111-125.

Pfaffl, M. W. (2001). A new mathematical model for relative quantification in real-time RT-PCR. *Nucleic Acids Res.* **29**, e45.

Pierce, R. A., Griffin, G. L., Susan Mudd, M., Moxley, M. A., Longmore, W. J., Sanes, J. R., Miner, J. H. and Senior, R. M. (1998). Expression of laminin alpha 3, alpha 4, and alpha 5 chains by alveolar epithelial cells and fibroblasts. *Am. J. Respir. Cell Mol. Biol.* **19**, 237-244.

Pierce, R. A., Griffin, G. L., Miner, J. H. and Senior, R. M. (2000). Expression patterns of laminin alpha 1 and alpha 5 in human lung during development. *Am. J. Respir. Cell Mol. Biol.* **23**, 742-747.

Rosenfeld, M. A., Yoshimura, K., Trapnell, B. C., Yoneyama, K., Rosenthal, E. R., Dalemans, W., Fukayama, M., Bargon, J., Stier, L. E., Stratford-Perricaudet, L. et al. (1992). In vivo transfer of the human cystic fibrosis transmembrane conductance regulator gene to the airway epithelium. *Cell* **68**, 143-155.

Ryan, M. C., Lee, K., Miyashita, Y. and Carter, W. G. (1999). Targeted disruption of the LAMA3 gene in mice reveals abnormalities in survival and late stage differentiation of epithelial cells. *J. Cell Biol.* **145**, 1309-1324.

Schuger, L., O'Shea, S., Rheinheimer, J. and Varani, J. (1990). Laminin in lung development: effects of anti-laminin antibody in murine lung morphogenesis. *Dev. Biol.* **137**, 26-32.

Trakala, M., Arias, C. F., García, M. I., Moreno-Ortiz, M. C., Tsilingiri, K., Fernández, P. J., Mellado, M., Díaz-Meco, M. T., Moscat, J., Serrano, M. et al. (2009). Regulation of macrophage activation and septic shock susceptibility <I>via</I> p21(WAF1/CIP1). *Eur. J. Immunol.* **39**, 810-819.

Tschumperlin, D. J. and Margulies, S. S. (1999). Alveolar epithelial surface area-volume relationship in isolated rat lungs. *J. Appl. Physiol.* **86**, 2026-2033.

Vanoirbeek, J. A. J., Rinaldi, M., De Vooght, V., Haenen, S., Bobic, S., Gayan-Ramirez, G., Hoet, P. H. M., Verbeken, E., Decramer, M., Nemery, B. et al. (2010). Noninvasive and invasive pulmonary function in mouse models of obstructive and restrictive respiratory diseases. *Am. J. Respir. Cell Mol. Biol.* **42**, 96-104.

Villar, J., Cabrera, N., Casula, M., Flores, C., Valladares, F., Muros, M., Blanch, L., Slutsky, A. and Kacmarek, R. (2010). Mechanical ventilation modulates Toll-like receptor signaling pathway in a sepsis-induced lung injury model. *Intensive Care Med.* **36**, 1049-1057.

Vlahakis, N. E. and Hubmayr, R. D. (2005). Cellular stress failure in ventilator-injured lungs. *Am. J. Respir. Crit. Care Med.* **171**, 1328-1342.

Weibel, E. R. (1963). *Morphometry of the Human Lung*. New York: Academic Press.

Weinberg, F., Hamanaka, R., Wheaton, W. W., Weinberg, S., Joseph, J., Lopez, M., Kalyanaraman, B., Mutlu, G. M., Budinger, G. R. S. and Chandel, N. S. (2010). Mitochondrial metabolism and ROS generation are essential for Kras-mediated tumorigenicity. *Proc. Natl. Acad. Sci USA* **107**, 8788-8793.

Whittaker, P., Kloner, R. A., Boughner, D. R. and Pickering, J. G. (1994). Quantitative assessment of myocardial collagen with picrosirius red staining and circularly polarized light. *Basic Res. Cardiol.* **89**, 397-410.

Willem, M., Miosge, N., Halfter, W., Smyth, N., Jannetti, I., Burghart, E., Timpl, R. and Mayer, U. (2002). Specific ablation of the nidogen-binding site in the laminin γ1 chain interferes with kidney and lung development. *Development* **129**, 2711-2722.

Journal of Cell Science

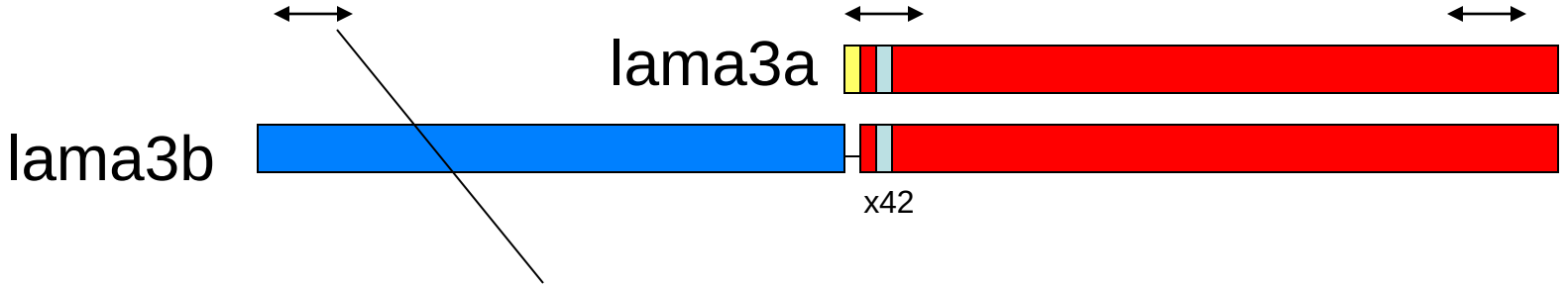

Lama3b specific

mlama3b 1F ACACCCTCCTCGGGCATCTTATTT
mlama3b 1R GCAGTTGCAGGCTTCACACTCATT
278bp

Lama3a specific

mlama3a 2F TATGGCTCAGAGCAGCAAAG
mlama3a/b 2R ACTGTGTTCCTGTGTATCCGGGTT
388bp

Lama3a AND lama3b

mLama3a/b 4F AGCACTTACGCTCACTCTCAGCAT
mLama3a/b 4R TTGGACATCGGTGGCTTCTGTGAT
433bp

Exon 42, excised in Cre treated mice

Supplemental Data Figure S1. Primer sequences to analyze knockdown of the α3 laminin gene. Schematic of the gene is found in the top panel, the arrows indicate the sites of the three primer sequences. Exon 42 (x42) is the site of the loxP sites. All values were normalizaed to GAPDH (Forward: 5'-AATGTGTCCGTCGTGGATCT) Reverse: 5'-CCCTGTTGCTGTAGCCGTAT)

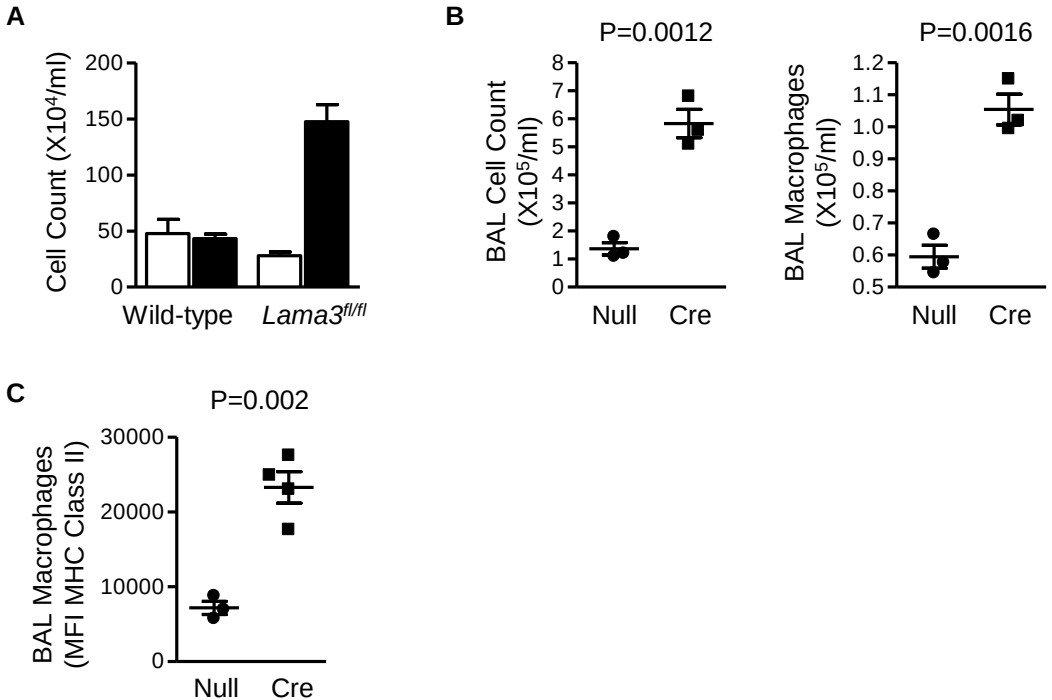

Supplemental Data Figure S2. Lung inflammation associated with the loss of α3 laminin. (**A**) Wild-type or *Lama3*$^{fl/fl}$ mice were treated Ad-Null or Ad-Cre and 60 days later a BAL was performed for measurement of total cell count (hemacytometer). (**B**) BAL fluid cells were quantified using flow cytometry, (**C**) Expression of the macrophage activation marker MHC Class II on BAL fluid macrophages was quantified using flow cytometry. Values above graphs indicate P values for comparison between Null and Cre. N $\geq$ 3 for all measures.

Blood

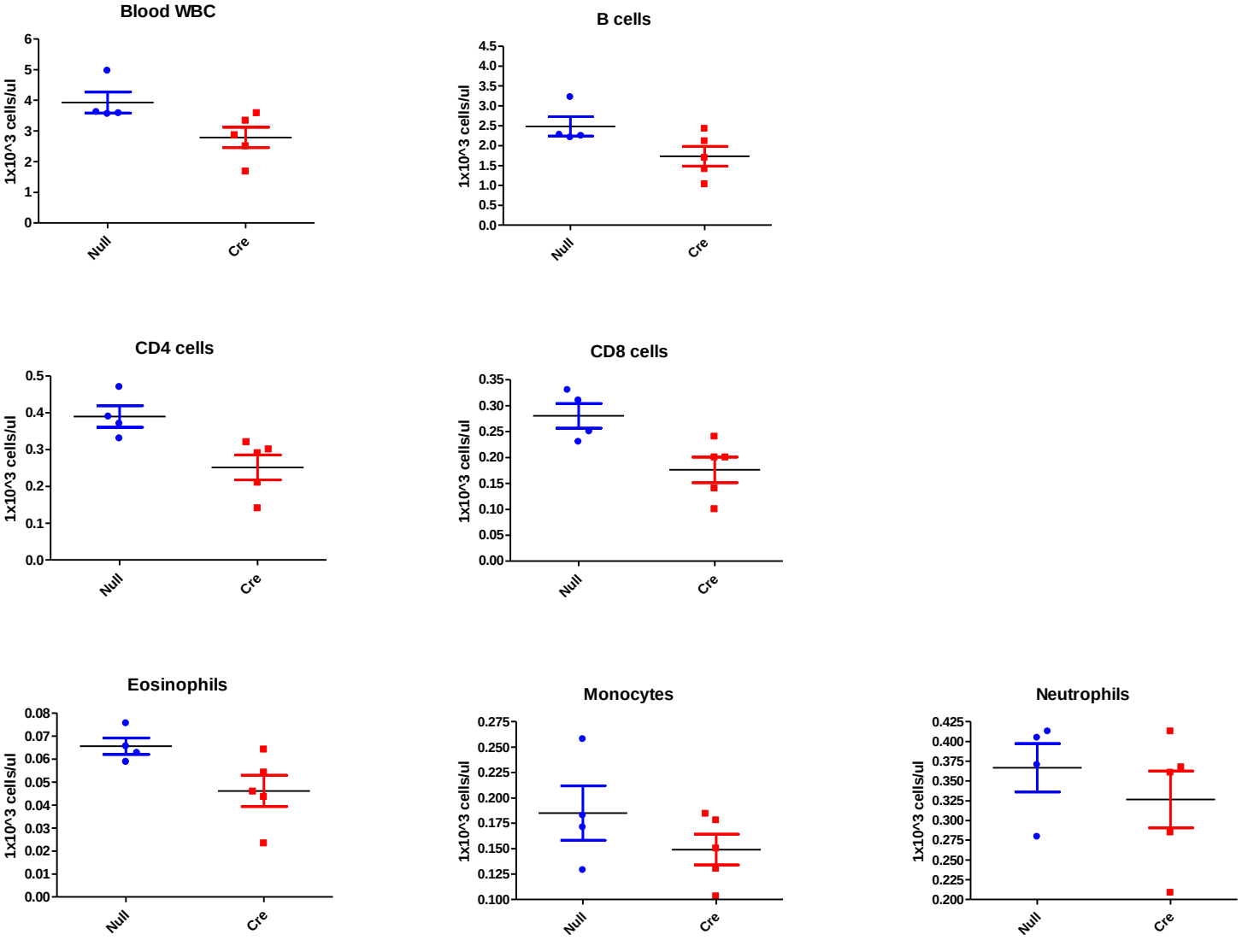

Supplemental Data Figure S3. Blood levels of inflammatory cells. (**A**) Wild-type or *Lama3*$^{fl/fl}$ mice were treated Ad-Null or Ad-Cre and 60 days later blood was collected for quantification of the leukocyte subsets indicated. N=3 for all measures, no statistically significant differences were observed between Null and Cre treated animals.

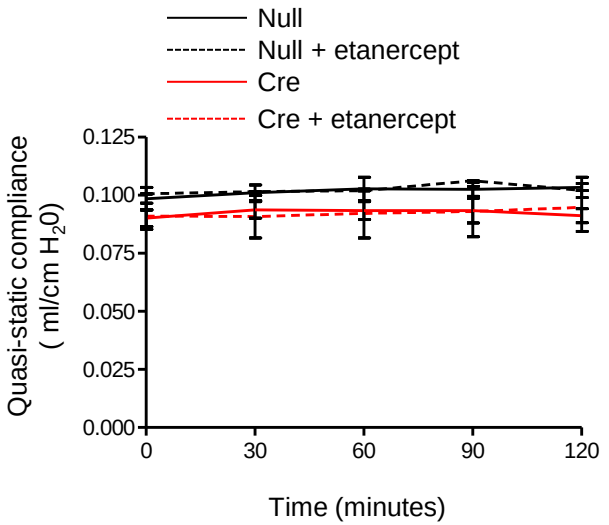

Supplemental Data Figure S4. Non-injurious ventilation does not alter lung compliance in wild-type or α3 laminin knockdown mice. *Lama3*$^{fl/fl}$ mice were treated with a null adenovirus (null) or an adenovirus encoding Cre recombinase (Cre) and 60 days later were subjected to 2 hours of non-injurious (V_T 12 ml/kg) mechanical ventilation using a flexivent ventilator (minute ventilation matched, PEEP = 0) and quasi-static lung compliance was assessed every 30 minutes during the mechanical ventilation.

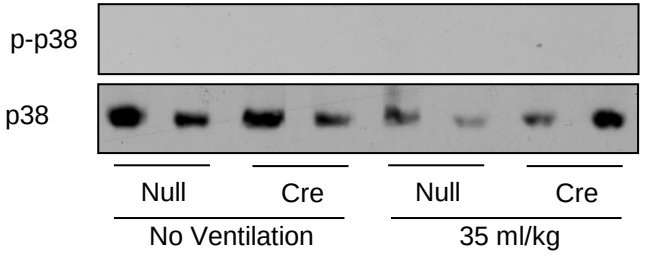

Supplemental Data Figure S5. No activation of p38 is detected in the lung following injurious ventilation. *Lama3*$^{fl/fl}$ mice were treated with a null adenovirus (Null) or an adenovirus encoding Cre recombinase (Cre) and 60 days later were untreated or subjected to injurious (V_T 35 ml/kg) mechanical ventilation using a flexivent ventilator (minute ventilation matched, PEEP = 0). After 20 mins, lung homogenates were immunoblotted using antibodies against phosphorylated and total p38, each lane represents a separate animal.

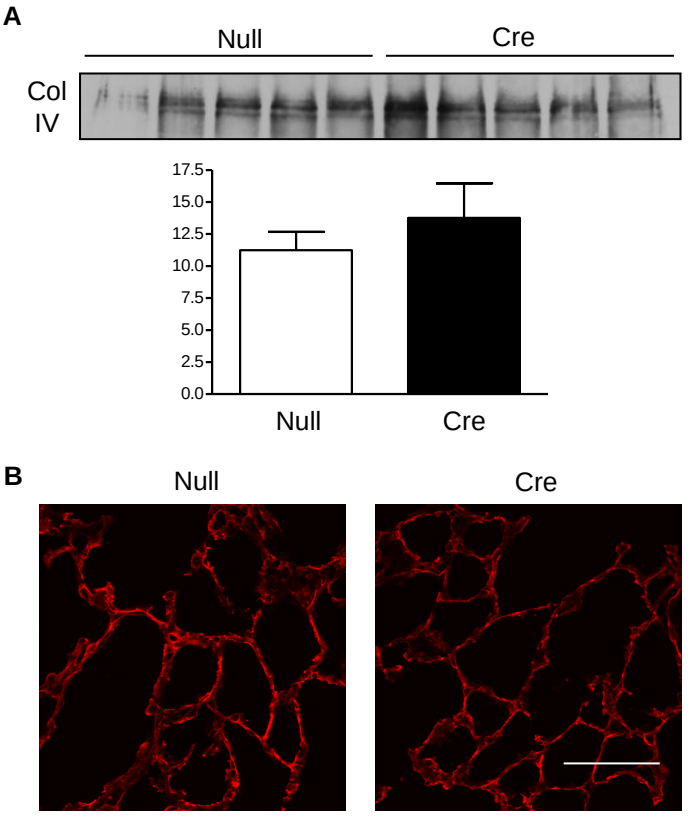

Supplemental Data Figure S6. Collagen IV is unchanged in Lama3 knockdown mice. *Lama3*$^{fl/fl}$ mice were treated with a null adenovirus (null) or an adenovirus encoding Cre recombinase (Cre) and (**A**) whole lung homogenates were obtained 60 days later and immunoblotted using an antibody against collagen IV. (**B**) Frozen lung sections were obtained from identically treated mice.

Table S1. Antibodies used for immunophenotyping

Cocktail 1: BAL and digested lung			
Marker	**Fluorochrome**	**Clone**	**Manufacturer**
CD45	PerCPCy5.5	30-11	BD Biosciences
CD11b	eFluor450	M1/70	eBioscience
CD11c	PECy7	HL3	BD Biosciences
F4/80	PETxRd	BM8	Invitrogen
Gr-1	APCCy7	RB6-8C5	BD Biosciences
CD40	Alexa Fluor 647	HM40-3	Biolegend
CD86	Alexa Fluor 700	GL1	BD Biosciences
CD62L	PE	MEL-14	BD Biosciences
MHC II	FITC	M5/114.15.2	BD Biosciences

Cocktail 2: Digested lung			
Marker	**Fluorochrome**	**Clone**	**Manufacturer**
CD45	PerCPCy5.5	30-11	BD Biosciences
CD11b	eFluor450	M1/70	eBioscience
CD11c	PECy7	HL3	BD Biosciences
Ly6C	FITC	AL21	BD Biosciences
Ly6G	PE	1A8	BD Biosciences
B220	PETxRd	RA3-6B2	BD Biosciences
CD3	APC	145-2C11	BD Biosciences
CD4	Pacific Orange	RM4-5	BD Biosciences
CD8	APCCy7	53-6.7	BD Biosciences
NK1.1	Alexa Fluor 700	PK136	BD Biosciences

Cocktail 3: Blood			
Marker	**Fluorochrome**	**Clone**	**Manufacturer**
CD45	Pacific Orange	30-11	BD Biosciences
CD11b	eFluor450	M1/70	eBioscience
Gr-1	FITC	RB6-8C5	BD Biosciences
CD115	PE	AFS98	eBioscience
B220	PETxRd	RA3-6B2	BD Biosciences
CD62L	APC	MEL-14	BD Biosciences
CD4	PerCPCy5.5	RM4-5	BD Biosciences
CD8	APCCy7	53-6.7	BD Biosciences
NK1.1	Alexa Fluor 700	PK136	BD Biosciences

Table S2. BD LSR II instrument configuration

Laser	PMT Slot	Filter	Mirror	Channel
Blue (488nm)/FSC	A	710/50	685LP	PerCPCy5.5
	B	525/50	505LP	FITC
	C	488/10		SSC
Red (640nm)	A	780/60	735LP	APCCy7
	B	730/745	690LP	Alexa Fluor 700
	C	670/30		APC/Alexa Fluor 647
Yellow-green (561nm)	A	780/60	735LP	PECy7
	B	610/20	600LP	PETexas Red
	C	582/15		PE
Violet (405nm)	A	582/15	570LP	Pacific Orange
	B	450/50		eFluor 450

Table S3. Definition of populations for flow cytometry

Alveolar macrophages	$CD45^{+}CD11c^{+}F4/80^{intermediate}CD11b^{intermediate}$
Neutrophils	$CD45^{+}CD11b^{high}Gr\text{-}1^{high}SSC^{high}$ or $CD45^{+}CD11b^{high}Ly6G^{+}$
$Ly6C^{high}$ Interstitial monocytes/macrophages	$CD45^{+}CD11b^{high}Gr\text{-}1^{intermediate}$ or $CD45^{+}CD11b^{high}Ly6C^{high}$ $Ly6G^{negative}$
$Ly6C^{low}$ Interstitial monocytes/macrophages	$CD45^{+}CD11b^{high}Gr\text{-}1^{low/negative}MHC\ II^{+}$ or $CD45^{+}CD11b^{high}Ly6C^{low/negative}$ $Ly6G^{negative}MHC\ II^{+}$
B cells	$CD45^{+}CD11b^{-}B220^{+}$
CD8 T cells	$CD45^{+}CD11b^{-}CD3^{+}CD8^{+}$

Table S4. Primer sequences for qRT-PCR

	Forward	**Reverse**
Lama3 gene	CCCAACCTGAGATTACAAGCA	CCAAAACCAAACATACCCCA
mlama3b	ACACCCTCCTCGGGCATCTTATTT	GCAGTTGCAGGCTTCACACTCATT
mlama3a	TGGTCAACACATGTCCCTCATCCA	ACTGTGTTCCTGTGTATCCGGGTT
mLama3a/b	AGCACTTACGCTCACTCTCAGCAT	TTGGACATCGGTGGCTTCTGTGAT
GAPDH	AATGTGTCCGTCGTGGATCT	CCCTGTTGCTGTAGCCGTAT